J. of Electromagn. Waves and Appl., Vol. 25, 527–538, 2011

STACKED PATCH ANTENNA ARRAY ON LTCC SUBSTRATE OPERATED AT 28 GHz

K.-S. Chin, H.-T. Chang, J.-A. Liu, B.-G. Chen, J.-C. Cheng and J. S. Fu

Chang Gung University
Taoyuan 333, Taiwan, R.O.C.

Abstract—This study develops a 28-GHz patch antenna array using LTCC (Low Temperature Co-fired Ceramic) technology, for use in applications of LMDS (Local Multipoint Distribution Service). The design comprises 2×2 stacked patch elements and parallel-fed networks, yielding a wide bandwidth and superior gain performance. Broadband performance is achieved by varying the dimensions of the parasitic patch. The arrays are excited through using a novel opposite-side feeding structure to prevent any electrical effect on the parasitic patch. Measurements correlate closely with the simulation results: a gain of 10.35 dBi and a bandwidth of 2.85 GHz (26.75–29.6 GHz) are achieved.

1. INTRODUCTION

Millimeter wave communication systems in 27.5–28.35 GHz, 29.1–29.25 GHz, 31.075–31.225 GHz, 31–31.075 GHz, and 31.225–31.3 GHz bands are being developed for use in LMDS (Local Multipoint Distribution Service) to provide reliable digital voice, data, and internet services [1–5]. LMDS depends on antennas to operate in the Ka band over a large bandwidth. Designing such antennas is difficult. Rectangular patch antennas are favored for their low profile, light weight, low cost, and ease of manufacture. However, they have the shortcoming of a narrow bandwidth because of their resonant behavior. Their low gain is also a major drawback, which must be overcome.

In recent years, LTCC (Low Temperature Co-fired Ceramic) has become an attractive multi-layer material, and is particular effective for use in high-frequency circuits that are required in high-speed data

Received 27 October 2010, Accepted 26 November 2010, Scheduled 4 January 2011
Corresponding author: Kuo-Sheng Chin (kschin@mail.cgu.edu.tw).

communications [5, 6, 9, 10, 12–17]. Stacked patch antennas [5–12] are well-known to have a large antenna bandwidth, which makes them very useful. Parasitic patches vertically above the main patch (also called the driven patch) are coupled electromagnetically in multi-layer structures to yield wideband characteristics. In one investigation [5], a method for designing stacked patch antennas with optimal bandwidth performance by varying the thickness of the LTCC substrate was developed. Panther et al. [6] utilized an embedded air cavity between stacked patches in LTCC devices to reduce the dielectric constant and quality factor to increase bandwidth. Byun et al. designed an 8×8 stacked patch antenna array that was backed by a metal cavity, yielding a large bandwidth [9]. One study [10] presented a slot-fed stacked patch antenna, with antenna feeding performed differentially via two pins. Another investigation [12] proposed a novel waveguide-to-microstrip transition to couple the stacked patch antenna array to the transceiver module at 40 GHz. However, the design of a compact stacked patch antenna array with large bandwidth and high gain is an ongoing challenge.

In this study, a 28 GHz patch antenna array that comprises 2×2 stacked patches in LTCC is designed for LMDS applications. Broadband performance is achieved by varying the dimensions of the parasitic patch. A novel opposite-side feeding structure is designed to draw out the embedded feed line for connection. The proposed antenna array has a wide bandwidth of up to 10.1%, with a superior gain of 10.35 dBi. An experimental antenna array was fabricated and measurements of it were made for demonstration purposes.

2. SINGLE-STACKED PATCH ANTENNA IN LTCC SUBSTRATE

Figures 1(a) and (b) display the 3D schematic structure and the cross-sectional configuration of a single stacked patch antenna in LTCC with a microstrip feed line. The operation of the stacked patches having a wideband performance will now be explained below. The equivalent circuit of the stacked patches is shown in Fig. 1(c), in which two coupled parallel RLC resonators are adopted establishing two resonance frequencies [18, 19]. The TM mode couples the main patch to an upper patch making its circuit response more inductive, and the parameter $M = m(L_1 \times L_2)^{1/2}$ denotes the magnetic-coupling inductance between the two patches, where m is a coupling coefficient. Fig. 1(d) plots the simulated S_{11} responses of the equivalent circuit in Fig. 1(c) with various m, using AWR's Microwave Office software with the assumed parameters listed in the caption of Fig. 1(d). This

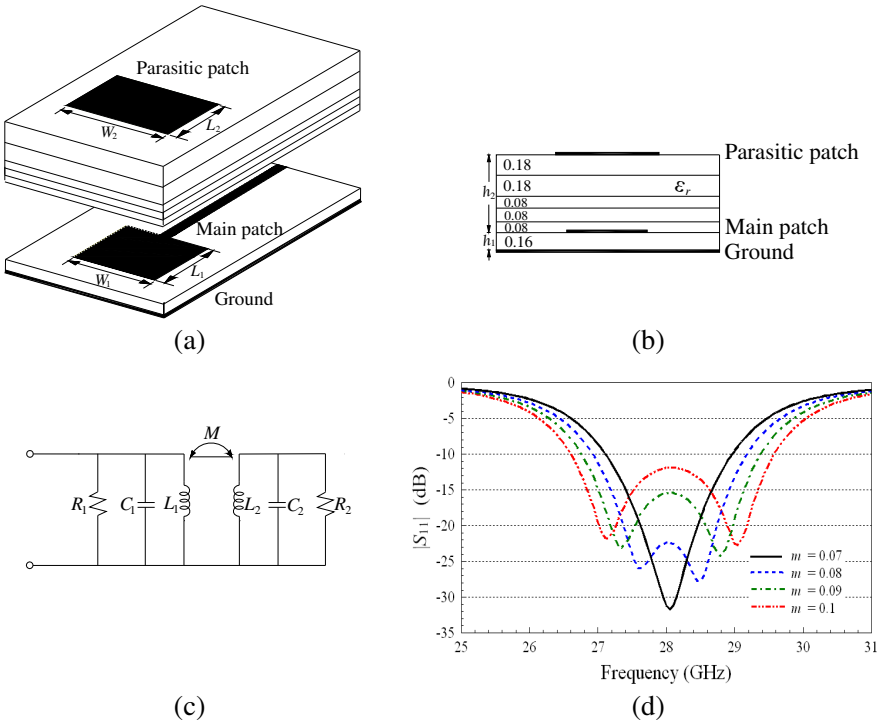

Figure 1. Single stacked patch antenna: (a) 3D schematic structure, (b) cross-sectional configuration, (c) equivalent circuit, and (d) simulated S_{11} responses ($L_1 = 0.02374\,\text{nH}$, $C_1 = 1.361\,\text{pF}$, $L_2 = 0.0959\,\text{nH}$, $C_2 = 0.337\,\text{pF}$, and $R_1 = R_2 = 200\,\Omega$ are assumed).

figure shows that the two resonant poles caused by the resonators $R_1L_1C_1$ (Main patch) and $R_2L_2C_2$ (Parasitic patch) can be pulled away using inductive coupling to achieve wideband characteristics. In practical design, the coupling coefficient m can be realized by varying the dimensions of the parasitic patch. Because the depth of return loss also decreases as m increases, it must account for the trade-offs between the required bandwidth and return loss performance. Notably, Fig. 1(d) was used only to characterize the variance in bandwidth associated with the inductive coupling scheme. The dimensions of the final antenna were finely tuned with the aid of the full-wave electromagnetic simulator HFSS.

The proposed antenna array consists of 2×2 stacked patch antenna elements to provide high gain and wide bandwidth. The circuit dimensions of a single stacked patch antenna must be determined first to verify the radiating characteristics before many of them are used

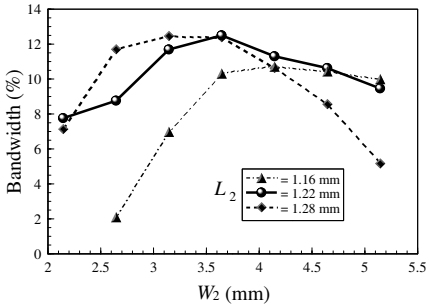

Figure 2. Bandwidth versus width of parasitic patches, W_2 for various lengths, L_2.

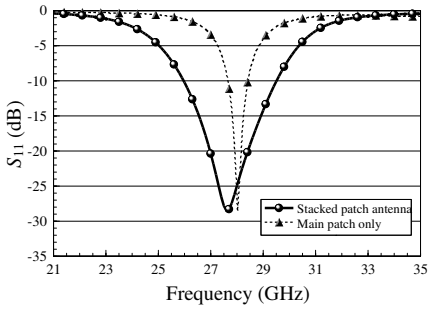

Figure 3. Simulated S_{11} parameter of single stacked patch antenna.

to form an array. This design adopts six ceramic layers to yield the required thickness; the parasitic patch and main patch are placed on the first and sixth ceramic layers, respectively. To keep the dielectric losses low, the LTCC material system, provided by Advanced Ceramic X Corporation (ACX), with a relative permittivity of $\varepsilon_r = 7.5$ and a loss tangent of $\tan\delta = 0.005$, are utilized. All buried and exposed conductors are silver. Based on the well-known design formulas [18–21], the main patch had dimensions of $L_1 = 1.78\,\text{mm}$, $W_1 = 1.845\,\text{mm}$, and $h_1 = 0.16\,\text{mm}$ (or $0.166\lambda_o$ by $0.172\lambda_o$ by $0.015\lambda_o$, where λ_o is the free-space wavelength) for operation at 28 GHz. The width of the feed line is set to 0.187 mm to realize a $50\,\Omega$ input impedance of the main patch. Fig. 2 plots the antenna bandwidth against the width of parasitic patches W_2 with various lengths L_2, but fixed $h_2 = 0.6\,\text{mm}$. As shown in Fig. 2, the bandwidth increases with W_2 and L_2 when $W_2 < 3.7\,\text{mm}$. Fig. 2 reveals that stacked patches with different sizes support a large bandwidth, and a maximum bandwidth of 12.6% is achieved when $W_2 = 3.645\,\text{mm}$ and $L_2 = 1.22\,\text{mm}$. Fig. 3 presents the simulated S_{11} response of a single stacked patch antenna, achieving a 10 dB impedance bandwidth of 12.6% (26 GHz to 29.5 GHz). For comparison, Fig. 3 also plots the corresponding curve of the main patch alone which only has a very narrow bandwidth of 3%.

3. PARALLEL FEEDING NETWORK AND OPPOSITE-SIDE FEEDING STRUCTURE

With respect to the integration of the 2×2 antenna elements, Fig. 4 plots the impedance arrangement of the proposed array feeding network. The 2D parallel feeding network is composed of power

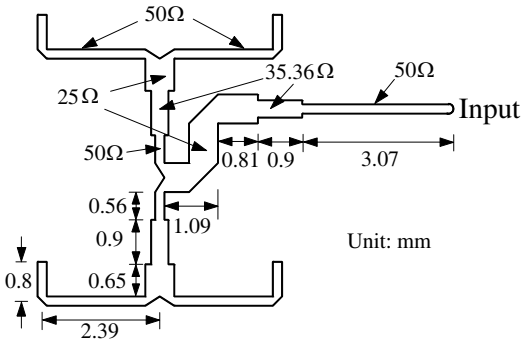

Figure 4. Impedance arrangement of 2×2 array parallel feeding network.

dividers and impedance transformers with three impedances of $50\,\Omega$, $35.36\,\Omega$, and $25\,\Omega$. The detail lengths of the parallel feeding network are also given in Fig. 4.

To test the performance of the antennas, the embedded feed line of the main patch must be drawn out from within the LTCC to the surface for connection. Accordingly, a good vertical interconnection between the input port and the main patch connection is required to allow good signal transmission. Moreover, the feed line should be separated from the parasitic patch to avoid any disturbance of the radiation patterns.

Figures 5(a) and (b) display a novel opposite-side feeding structure, which does not electrically influence the parasitic patch, because it is situated on the opposite side and separated by a ground. The upper feed line (port 2, to main patch) is connected to the lower feed line (port 1, to connector) using a signal via which is lined on both sides with ground vias to construct a vertical ground-signal-ground (G-S-G) structure Many ground vias are applied to connect ground planes (on the first, second, and sixth ceramic layers) to equalize the ground potential. An aperture on the bottom ground (on the sixth ceramic layer) with a radius of 0.35 mm is etched allowing the signal via and the lower feed line to pass through it without touching. To maintain the 50-Ω impedance of the feed lines, the required width of the lower feed line increases with the substrate, potentially causing discontinuity effects. Therefore, the ground above the lower feed line must be leveled down to reduce the width of the lower feed line to ensure a good interconnection. In the authors' studies, 0.48 mm was an appropriate width for the lower feed line. Fig. 5(c) plots the simulated S-parameter responses of the proposed opposite-side feeding structure obtained by treating it as a two-port network. Excellent insertion loss is observed with $|S_{21}| < 0.9\,\text{dB}$ at 28 GHz, while $|S_{11}| > 12\,\text{dB}$.

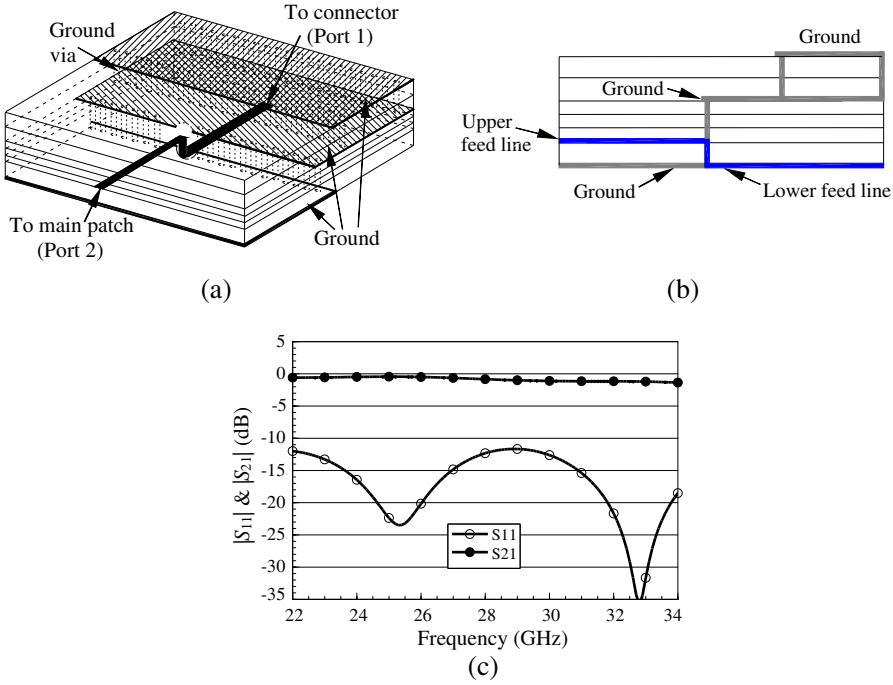

Figure 5. (a) 3D schematic structure, (b) cross-sectional configuration and (c) simulated S-parameter responses, of the opposite-side feeding structure.

4. 2 × 2 STACKED PATCH ANTENNA ARRAY FABRICATION AND MEASUREMENTS

A 2×2 stacked patch antenna array operated at 28 GHz was synthesized on an LTCC substrate to validate the design approach. The full-wave electromagnetic simulator Ansoft HFSS was used in the simulation. Fig. 6(a) presents the 3D schematic structure of the proposed 2 × 2 stacked patch antenna array with an opposite-side feeding structure, in which the unseen feed line is located at the bottom surface of the antenna. Figs. 6(b) and (c) show the circuit dimensions and the thickness of the layers, respectively.

Figure 7 plots the simulated and measured S_{11} responses. The measurements of S_{11} reveal that the central frequency shifted slightly to 28.18 GHz with a 10 dB impedance bandwidth of 10.1% (26.75–29.6 GHz). Figs. 8(a) and 8(b), 8(c) and 8(d), 8(e) and 8(f) present the xz-plane and yz-plane radiation patterns at 26.75 GHz, 28 GHz,

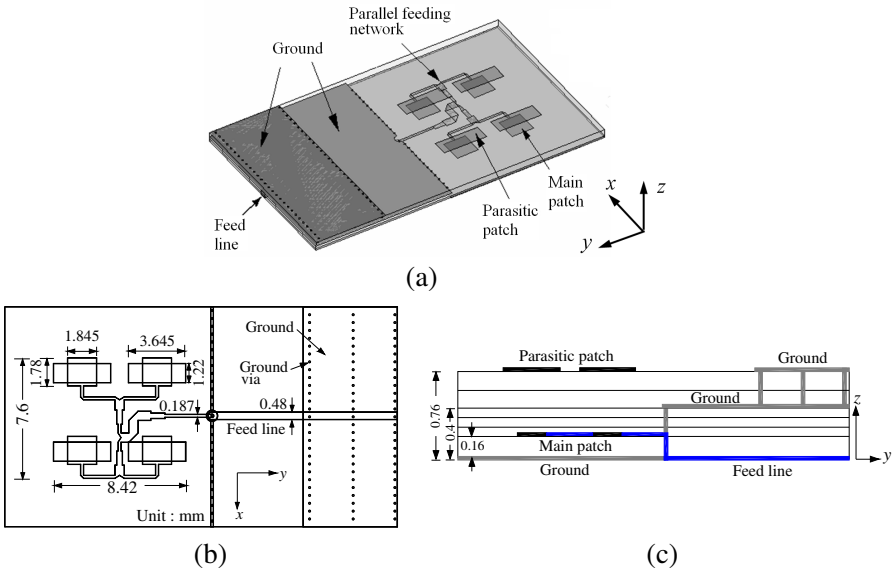

Figure 6. Proposed 2×2 stacked patch antenna array with 2D parallel feeding network and opposite-side feeding structure: (a) 3D schematic structure, (b) dimensions, and (c) thickness of layers, of the array.

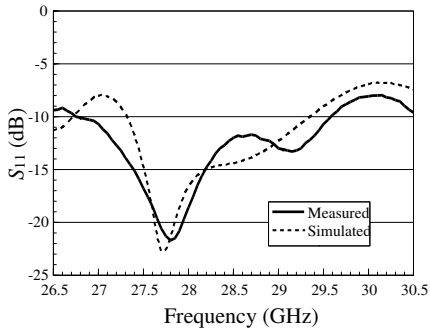

Figure 7. Simulated and measured S_{11} responses of 2 × 2 stacked patch antenna array.

and 29.6 GHz, respectively, measured in a far-field anechoic chamber. As these figures show, the radiation patterns at the three frequencies have very similar shape in the angle range of −45° to +45°. Notably, the asymmetry in the *xz*-plane and *yz*-plane radiation patterns is mainly caused by the parallel feeding network and ground planes.

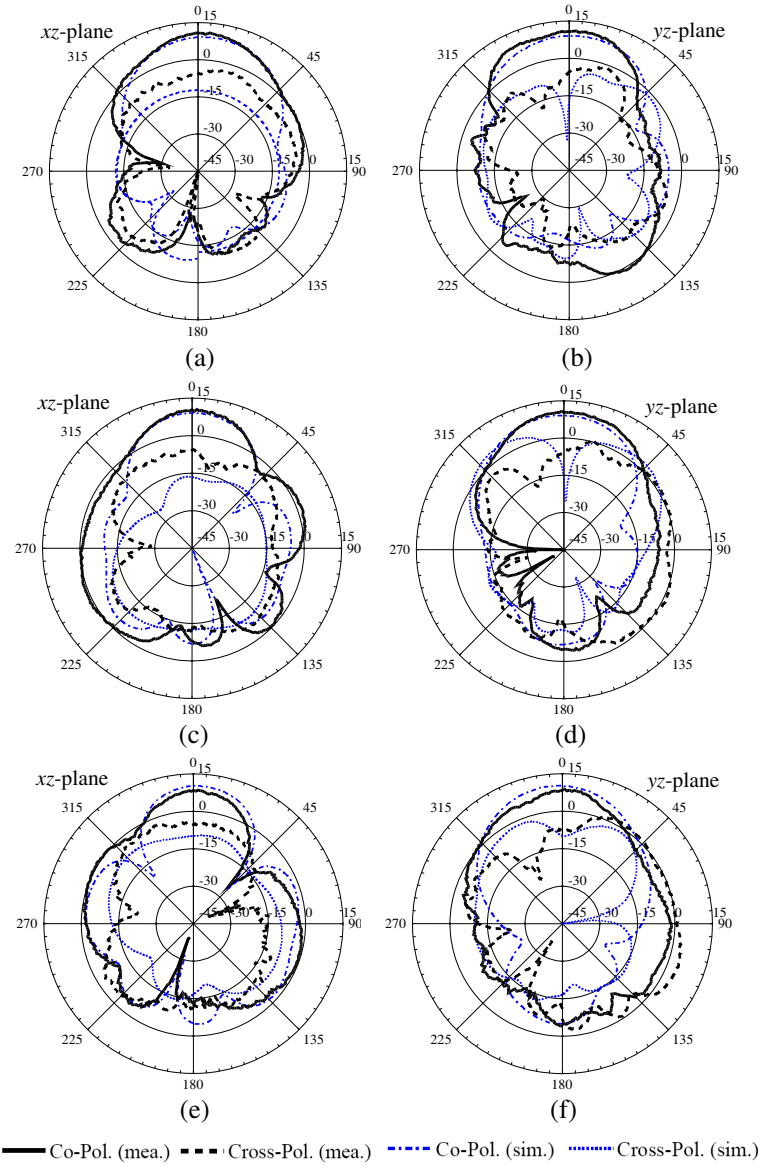

Figure 8. Simulated and measured radiation patterns of experimental array: (a) 26.75-GHz xz-plane, (b) 26.75-GHz yz-plane, (c) 28-GHz xz-plane, (d) 28-GHz yz-plane, (e) 29.6-GHz xz-plane, and (f) 29.6-GHz yz-plane.

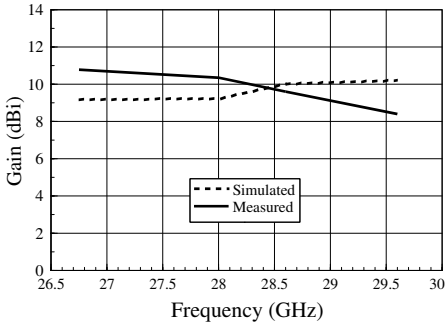

Figure 9. Measured and simulated antenna gain in range 26.75–29.6 GHz.

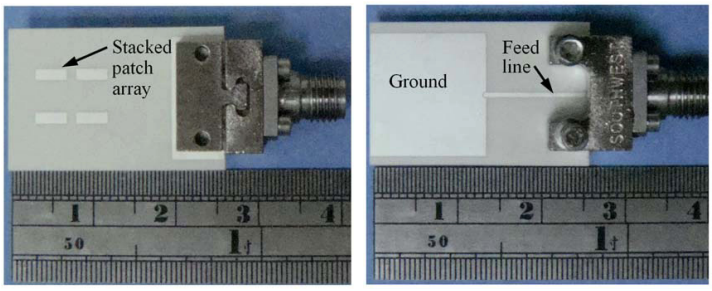

(a) (b)

Figure 10. (a) Top-view photograph and (b) bottom-view photograph, of fabricated 2×2 stacked patch antenna array with an attached K end-launch connector for testing.

From Figs. 8(c) and (d), the xz-plane and yz-plane have smooth co-polarization patterns with half-power beamwidths of 36° and 48°, respectively, and a gain of 10.35 dBi at 28 GHz. The cross-polarization measurements are better than −5.7 dBi in the 0° direction.

Figure 9 plots the measured and simulated gain of the fabricated antenna in the range 26.75–29.6 GHz. The measured gain varies within 2.38 dB (10.78–8.4 dB) over the entire band. All these results include the effect of the K end-launch connector, and are favorable for patch antennas that are operated at such a high frequency. The deviation in measured gain was mainly caused by the insufficient connection of the feed line and the K end-launch connector, especially for operation at high frequencies. The other possibility is inaccuracy in both polarization and mechanical alignment between the transmitting horn and the experimental antenna array. All of these problems could be

overcome by modifying the feed design and increasing the accuracy of positioning. Figs. 10(a) and (b) are photographs of the experimental 2×2 stacked patch antenna array. The overall size, excluding the connector, is 2.6 cm $\times$ 1.65 cm $\times$ 0.76 mm.

5. CONCLUSION

In this study, 2×2 stacked patch antenna arrays are designed for LMDS band applications. The antennas comprise 2×2 stacked patch elements in LTCC to raise gain. Wideband performance is achieved by varying the dimensions of the parasitic patch. This investigation develops a novel opposite-side feeding structure for connection. The design concept was demonstrated by fabricating an experimental stacked patch antenna array that yielded a bandwidth of 10.1% and a gain of 10.35 dBi. Because the required fabrication accuracy is very easy to achieve using the general LTCC fabrication process, the proposed stacked patch antenna array can be produced with more consistently stable performance. For future applications in wireless systems, it is possible to integrate with the slotted patch and the differential feeding structure to achieve much wider bandwidth and low cross-polarization performance.

ACKNOWLEDGMENT

This work was partially supported by the National Science Council, Taiwan, R.O.C., (NSC 99-2221-E-182-033) and Chang Gung University, Taiwan, R.O.C., (UERPD290051). The authors would also like to acknowledge the support of High Speed Intelligent Communication (HSIC) Research Center, Chang Gung University.

REFERENCES

1. Arrebola, M., J. A. Encinar, and M. Barba, "Multifed printed reflectarray with three simultaneous shaped beams for LMDS central station antenna," *IEEE Trans. Antennas Propag.*, Vol. 56, No. 6, 1518–1527, June 2008.
2. Chen, K.-S. and C.-Y. Chu, "A propagation study of the 28 GHz LMDS system performance with M-QAM modulations under rain fading," *Progress In Electromagnetics Research*, Vol. 68, 35–51, 2007.
3. Oh, S., S. Seo, M. Yoon, C. Oh, E. Kim, and Y. Kim, "A

broadband microstrip antenna array for LMDS applications," *Microw. Optical Tech. Lett.*, Vol. 32, 3537, January 2002.

4. Lee, H., T. Kim, and Y. Lim, "Wide-band microstrip patch antenna design for LMDS band," *International Symposium on Antennas, Propagation and EM Theory*, 709–712, 2002.
5. Rong Lin, L., G. DeJean, M. Moonkyun, L. Kyutae, S. Pinel, M. M. Tentzeris, and J. Laskar, "Design of compact stacked-patch antennas in LTCC multilayer packaging modules for wireless applications," *IEEE Trans. on Advanced Packaging*, Vol. 27, No. 24, 581–589, November 2004.
6. Panther, A., A. Petosa, M. G. Stubbs, and K. Kautio, "A wideband array of stacked patch antennas using embedded air cavities in LTCC," *IEEE Microw Wireless Compon Lett.*, Vol. 15, 916–918, 2005.
7. Vázquez, C., G. Hotopan, S. V. Hoeye, M. Fernández, L. F. Herrán, and F. L. Heras, "Microstrip antenna design based on stacked patches for reconfigurable two dimensional planar array topologies," *Progress In Electromagnetics Research*, Vol. 97, 95–104, 2009.
8. Du, S., Q.-X. Chu, and W. Liao, "Dual-band circularly polarized stacked square microstrip antenna with small frequency ratio," *Journal of Electromagnetic Waves and Applications*, Vol. 24, No. 11–12, 1599–1608, 2010.
9. Byun, W. J., K. C. Eun, B. S. Kim, K. S. Kim, and M. S. Song, "Design of 8×8 stacked patch array antenna on LTCC substrate operating at 40 GHz band," *Asia Pacific Microwave Conference*, 2634–2637, 2005.
10. Valavan, A. S. E., B. Yang, A. Yarovoy, and L. P. Ligthart, "An M-band differentially fed, aperture coupled stacked patch antenna in LTCC," *Proceeding of the 5th European Radar Conference*, 200–203, 2008.
11. Losada, V., R. R. Boix, and F. Medina, "Resonant modes of stacked circular microstrip patches in multilayered substrates containing anisotropic and chiral materials," *Journal of Electromagnetic Waves and Applications*, Vol. 17, No. 4, 619–640, 2003.
12. Byun, W., B.-S. Kim, K.-S. Kim, and M.-S. Song, "LTCC microstrip patch array antenna with WR-22 feeding structure for an integrated transceiver module," *IEEE Antennas and Propagation Society Symposium*, 1495–1498, 2006.
13. Lamminen, A. E., J. Säily, and A. R. Vimpari, "60-GHz patch antennas and arrays on LTCC with embedded-cavity substrates," *IEEE Trans. Antennas Propag.*, Vol. 56, 2865–2874, 2008.

14. Xia, L., R. Xu, and B. Yan, "LTCC interconnect modeling by support vector regression," *Progress In Electromagnetics Research*, Vol. 69, 67–75, 2007.
15. Wang, Z., P. Li, R. Xu, and W. Lin, "A compact X-band receiver front-end module based on low temperature co-fired ceramic technology," *Progress In Electromagnetics Research*, Vol. 92, 167–180, 2009.
16. Zhang, Y. P. and D. Liu, "Antenna-on-chip and antenna-in-package solutions to highly integrated millimeter-wave devices for wireless communications," *IEEE Trans. Antennas Propag.*, Vol. 57, 2830–2841, 2009.
17. Lopez-Berrocal, B., J. de-Oliva-Rubio, E. Marquez-Segura, A. Moscoso-Martir, I. Molina-Fernandez, and P. Uhlig, "High performance 1.8–18 GHz 10-dB low temperature co-fired ceramic directional coupler," *Progress In Electromagnetics Research*, Vol. 104, 99–112, 2010.
18. Garg, R., et al., *Microstrip Antenna Design Handbook*, Artech House, Norwood, MA, 2001.
19. James, J. R., et al., *Handbook of Microstrip Antennas*, Peter Peregrinus, London, United Kingdom, 1989.
20. Milligan, T. A., *Modern Antenna Design*, Jone Wiley & Sons, Hoboken, New Jersey, 2005.
21. Balanis, C. A., *Antenna Theory Analysis and Design*, 3rd edition, John Wiley & Sons, Hoboken, New Jersey, 2005.